The electronic and superconducting properties of ordered Ti-Rh alloys

1991 J. Phys.: Condens. Matter 3 1089

(http://iopscience.iop.org/0953-8984/3/9/006)

J. Phys.: Condens. Matter 3 (1991) 1089–1098. Printed in the UK

The electronic and superconducting properties of ordered Ti–Rh alloys

Andrzej Szajek
Institute of Molecular Physics of Polish Academy of Sciences, Smoluchowskiego 17/19, 60–179 Poznan, Poland

Received 25 May 1990, in final form 29 October 1990

Abstract. The LMTO ASA calculations have been performed for ordered Ti–Rh alloys: $TiRh_3$, Cu_3Au-type structure; TiRh, CsCl- and CuAuI-type structure. Using the electronic band-structure calculations the electron–phonon coupling parameter λ and the superconducting temperature T_c were calculated.

1. Introduction

The experimental information on the electronic properties of ordered Ti–Rh alloys has been obtained through the low-temperature specific heat and magnetic susceptibility measurements by Kuentzler and Waterstrat [1, 2]. These workers considered three crystallographic structures: Cu_3Au-, CuAuI- and $MoSi_2$-type structures. The conclusions from these studies are the following.

(i) No magnetic order and no superconductivity are observed in these systems above a temperature of 1.4 K.

(ii) The high-temperature CsCl-type structure transforms via a martensitic transformation to the CuAuI-type structure.

Other structural studies [3, 4] showed that TiRh alloy above 845 °C had a cubic CsCl-type structure. In the range from 845 to 83 °C this cubic structure transformed continuously to the tetragonal structure ($c/a = 1.00$–1.121). At a temperature of 83 °C the tetragonal CuAuI-type structure ($c/a = 0.79271178$) was found. At lower temperatures a distortion was observed and transition to the monoclinic symmetry (at 25 °C, $a = 4.178$ Å, $b = 4.185$ Å, $c = 3.371$ Å and $\gamma = 90.89°$).

In this paper we would like to consider three crystallographic systems of Ti–Rh alloys: Cu_3Au-, CsCl- and CuAuI-type structures. Some theoretical calculations were performed for similar systems earlier. Our previous calculations were devoted to the related Zr–Rh alloys [5]. Using the self-consistent linear muffin-tin orbitals (LMTO) method in the atomic sphere approximation (ASA) we have calculated the electronic structures for the three above-mentioned crystallographic structures. The electron–phonon coupling parameters λ were estimated by comparing the theoretical coefficients γ_0, and experimental coefficients γ of the electronic specific heat. Watson *et al* [6, 7] using self-consistent scalar-relativistic linear-augmented Slater-type orbitals (LASTOs) calculated the heats of formation for ordered compounds of Ti, Zr and Hf alloyed with Tc, Re, Ru, Os, Rh, Ir, Pd and Pt. The calculations have been done for sets of special

0953-8984/91/091089 + 10 $03.50

k-points in reciprocal space. The number of k-points was more than enough to establish the total energy and sufficient to define the general features of the density of states but the number of k-points was not, in general, sufficient for an accurate determination of the density of states at the Fermi level. Folkerts and Haas [8] have studied the relation between the electronic structure of TiRh and the transition from the high-temperature cubic CsCl structure to the tetragonal structure at 845 °C. The calculations were performed using the augmented spherical wave (ASW) method. The tetragonal structure had a lower total energy than the cubic structure. The calculations were performed for the cubic and tetragonal CsCl-type structures although these structures are not exactly the structures existing at the low temperatures. In fact, the CsCl-type structure transforms into the tetragonal structure owing to martensitic transformation [2, 3], which distorts continuously into a monoclinic structure below 83 °C. The organization of this paper is as follows. In section 2 we briefly present some details of electronic structure calculations. Section 3 includes the results of band calculations: energy bands and densities of states. In section 4 we calculate the electron–phonon coupling parameter λ and the transition temperatures to the superconducting phase for the two low-temperature structures CuAuI and Cu_3Au. Finally we summarize the results.

2. Method of band calculations

We have performed self-consistent electronic structure calculations for Ti–Rh ordered systems. Using the LMTO ASA method [9–11] the von Barth–Hedin [12] exchange–correlation potential was used. The following initial configurations for the calculations of the atomic charge densities were used: core + $3d^34s^1$ for titanium and core + $4d^85s^1$ for rhodium. The iterations were performed to self-consistency for the valence electrons only, and the core electrons were treated as frozen. Eigenvalues for all of the structures were calculated at 84 k-points in the irreducible wedge of the Brillouin zone and a step size of 1 mRyd was used to integrate the density of states (DOS). The tetrahedron method was used to evaluate the DOS [13, 14]. The position of the Fermi level is calculated with respect to the muffin-tin zero potential V_{MTZ}. In the LMTO ASA kinetic energy $\kappa^2 = E - V_{MTZ}$ in the interstitial region is chosen to be equal to zero [9–11]. The Wigner–Seitz cell is replaced by a sphere with radius S. The radius of the sphere is determined by the condition $4\pi S^3 n/3 = V$, where V is the volume of the Wigner–Seitz cell and n is the number of atoms in a primitive cell. The average sphere radii (the same for different types of atoms) for the systems have been obtained by minimizing the total energy in the paramagnetic phase.

3. Results of band-structure calculations

In this paper we shall consider cubic-type systems. The experimental data [3, 4] show the existence of the cubic structure Cu_3Au and tetragonal phases CsCl ($c/a > 1$) and CuAuI ($c/a < 1$). Recently Folkerts and Haas [8] showed on the basis of the ASW method that the tetragonal CsCl-type structure had a lower energy, by about 0.04 eV/unit cell than the cubic structure. Watson *et al* [6] using the LASTO method have calculated, among other things, the heats of formation for Ti–Rh systems. The calculations have shown that the heats of formation for the tetragonal CuAuI- and cubic CsCl-type structures are approximately equal. The cubic CuAuI structure had a higher energy than the tetragonal structure. Our calculations have shown that the cubic CuAuI structure has a higher energy, by 0.4814 Ryd/formula unit, than the cubic CsCl structure. Of the three considered systems the Cu_3Au-type structure has the largest total energy per atom. The

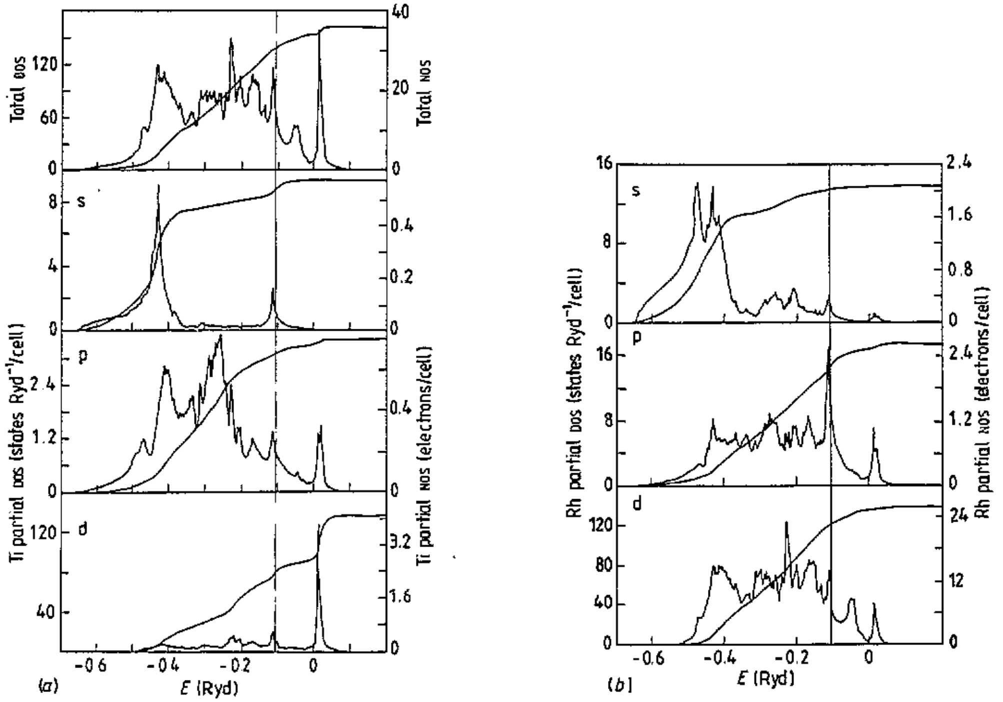

Figure 1. The total and partial DOS and NOS for $TiRh_3$ alloy. The vertical line describes the Fermi level.

Table 1. DOSs and NOSs at the Fermi level in $TiRh_3$ alloy and the bottom of bands for the particular angular momentum quantum numbers l ($TiRh_3$, $AuCu_3$-type structure; S = 2.885 au; $E_F = -0.1040$ Ryd).

	DOS (states Ryd^{-1} /cell)				NOS (electrons/cell)			
	s	p	d	Total	s	p	d	Total
$TiRh_3$	1.727	7.985	39.686	49.398	2.578	2.977	25.445	31.000
Ti	0.904	0.800	7.366	9.070	0.548	0.686	2.446	3.680
3Rh	0.823	7.185	32.320	40.328	2.030	2.291	22.999	27.320
	Bottom of bands (Ryd)							
	Ti s	Ti p	Ti d		Rh s	Rh p	Rh d	
	−0.649	−0.648	−0.640		−0.649	−0.649	−0.649	

charge transfer from rhodium to titanium and the DOS at Fermi level have the smallest values for the Cu_3Au structure. The DOS for $TiRh_3$ is very similar to that obtained in our previous calculations for $ZrRh_3$ [5] (figure 1). The main contribution to the DOS at the Fermi level is from the d electrons of rhodium and this is presented in table 1, together with the number of states (NOS). The Fermi level is located on the slope of peak near a DOS valley for $E_F = -0.1040$ Ryd. The band structure is presented in figure 2. The minimum of the total energy is obtained for $S = 2.885$ au which corresponds to a lattice

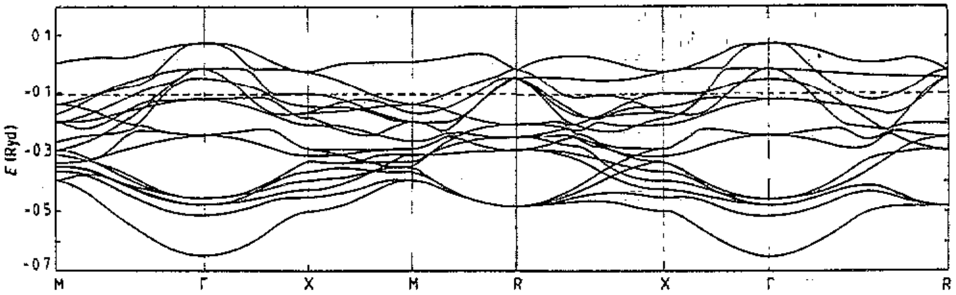

Figure 2. Dispersion curves along the high-symmetry directions for $TiRh_3$. The broken line represents the Fermi level.

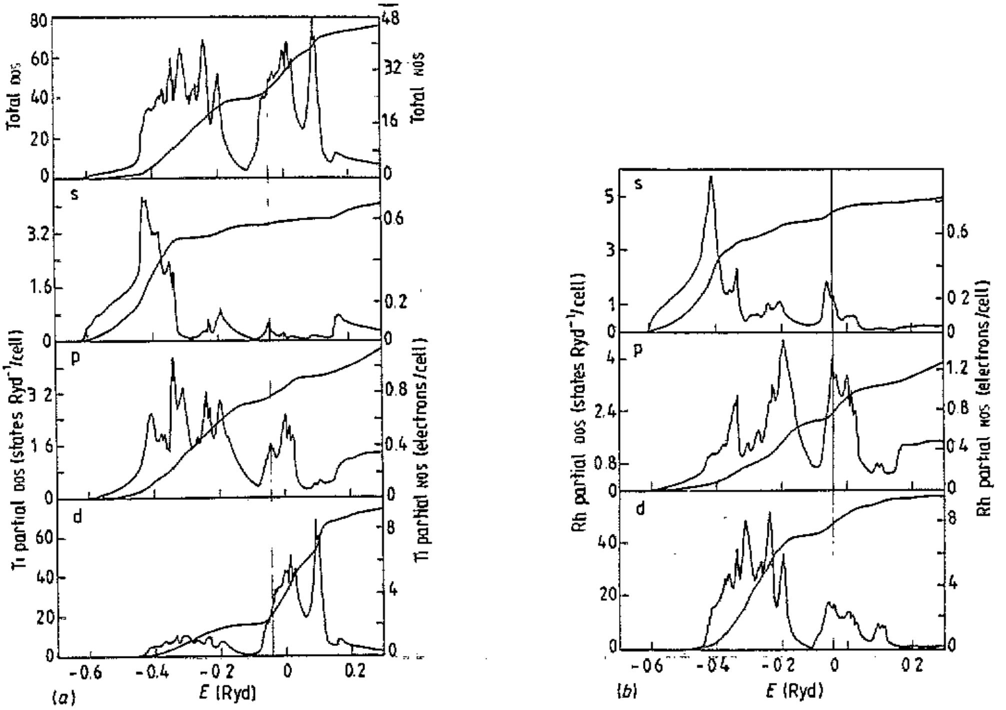

Figure 3. The total and partial DOS and NOS for TiRh alloy of CsCl-type structure. The vertical line describes the Fermi level.

constant equal to 3.9066 Å. The experimental value is less than the theoretical value by about 2% [4].

The shape of our DOS for the CsCl-type structure is very similar to that obtained by Folkerts and Haas [8]. The Fermi level is located at the same position on the left-hand slope of the part of DOS lying at higher energies. In this case the Fermi level is equal to −0.0524 Ryd (the DOS is given in figure 3 and the band structure in figure 4). The value of the radius S is 2.92 au and is larger by about 0.4% than the experimental high-temperature value [3]. The radii obtained by Folkerts and Haas [8] are also close to our values and the difference is about 0.7 and 1% for the cubic and tetragonal structures, respectively. The value of the DOS at Fermi level is much smaller (table 2) in our case. The value obtained by Folkerts and Haas [8] is equal to 62.56 states Ryd^{-1}/cell and our

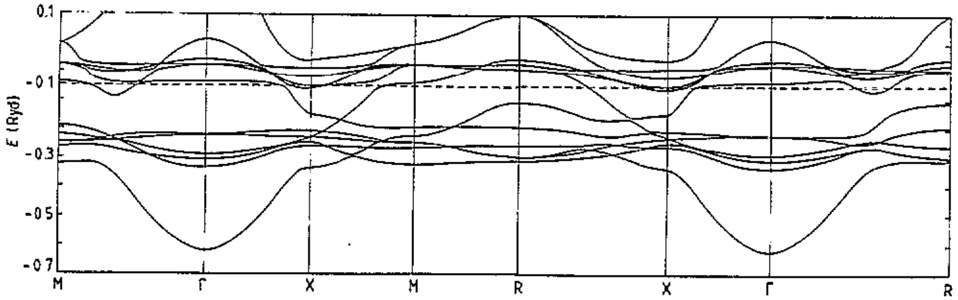

Figure 4. Dispersion curves along the high-symmetry directions for TiRh of cubic CsCl-type structure. The broken line represents the Fermi level.

Table 2. DOSs and NOSs at the Fermi level in TiRh alloy for CsCl-type structure alloy and the bottom of bands for the particular angular momentum quantum numbers l (TiRh, CsCl-type structure; $S = 2.920$ au; $E_F = -0.0524$ Ryd).

	DOS (states Ryd^{-1}/cell)				NOS (electrons/cell)			
	s	p	d	Total	s	p	d	Total
TiRh	1.724	3.928	34.253	39.905	1.310	1.494	10.196	13.000
Ti	0.327	1.245	17.823	19.395	0.577	0.748	2.425	3.750
Rh	1.397	2.683	16.430	20.510	0.733	0.746	7.771	9.250

Bottom of bands (Ryd)

Ti s	Ti p	Ti d	Rh s	Rh p	Rh d
−0.616	−0.615	−0.609	−0.616	−0.615	−0.611

value of 39.905 states Ryd^{-1}/cell is rather closer to the value of 43.52 states Ryd^{-1}/cell that they obtained for the tetragonal CsCl-type structure [8]. It is not easy to explain the reason for the difference between the value obtained by Folkerts and Haas and our value for the DOS at the Fermi level. The paper by Folkerts and Haas does not include information on the number of k-points used in integration over the Brillouin zone. Looking at their DOS it seems that too small a number of k-points could be responsible for this difference. There are many small sharp peaks in the DOS and the Fermi level is located close to such a small peak. To support our results (for 84 k-points) we have examined the convergence problem in our calculations.† The calculations for TiRh (CsCl structure) using 286 k-points in one forty-eighth of Brillouin zone gave similar results and finally $\Delta N(E_F) \simeq 0.5$ states Ryd^{-1}/cell.

In the case of the CuAuI-type structure the DOS is narrower and the peaks are much higher. The distance from the bottom of band to the Fermi level is smaller than for the CsCl-type structure. The DOS at the Fermi level is larger, $N(E_F) = 42.533$ states Ryd^{-1}/formula unit, although it lies at the deepest point, $E_F = -0.1517$ Ryd (a comparison of the Fermi energy position with the bottom of the bands is given in table 3, where other numerical values for this system are also included, the DOS shape is shown in figure 5 and the band structure is presented in figure 6). The radius of the Wigner–Seitz sphere in this structure is equal to 3.16 au. Usually the CuAuI-type structure is characterized by

---

† The author is grateful to the referee for the suggestion that we should check the convergence problem.

Table 3. DOSs and NOSs at the Fermi level in TiRh alloy for CuAu-type structure alloy and the bottom of bands for the particular angular momentum quantum numbers l (TiRh, CuAuI-type structure; $S = 3.160$ au; $E_F = -0.1517$ Ryd).

	DOS (states Ryd^{-1}/formula unit)				NOS (electrons/formula unit)			
	s	p	d	Total	s	p	d	Total
TiRh	5.237	3.578	33.718	42.533	1.867	0.685	10.448	13.000
Ti	3.819	0.944	27.269	32.032	0.834	0.374	2.321	3.529
Rh	1.418	2.634	6.449	10.501	1.033	0.311	8.127	9.471

Bottom of bands (Ryd)					
Ti s	Ti p	Ti d	Rh s	Rh p	Rh d
−0.618	−0.617	−0.607	−0.618	−0.617	−0.607

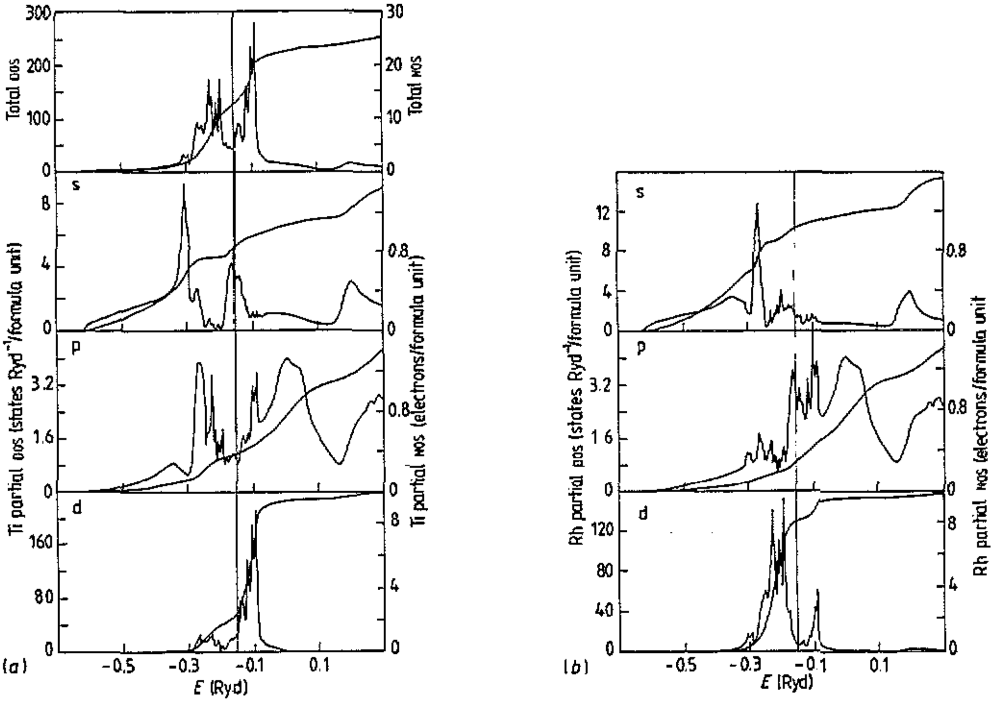

Figure 5. The total and partial DOS and NOS for TiRh alloy of CuAuI-type structure. The vertical line describes the Fermi level.

relatively high values of the DOS. For the related Zr–Rh alloys the DOS at the Fermi level in the CuAuI-type structure is about 23% larger than for the CsCl structure [5]. For Ti–Rh the difference is about 7% only. It could mean that the CuAuI-type structure for TiRh is more stable than the CuAuI-type structure for ZrRh compared with the CsCl-type structures. The probable change in symmetry from cubic to tetragonal, which is more stable at low temperatures, could reduce the total energy and the DOS at the Fermi level of the system. In both cases (CsCl- and CuAuI-type structures), the main

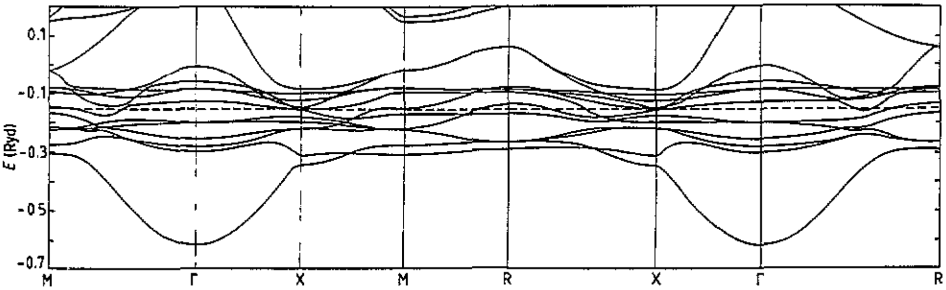

Figure 6. Dispersion curves along the high-symmetry directions for TiRh of cubic CuAuI-type structure. The broken line represents the Fermi level.

contribution to the DOS at the Fermi level is from the d electrons. The DOSs are divided by the Fermi level into two regions. The titanium contribution lies above E_F and the rhodium contribution below E_F.

The results of the band-structure calculations presented in this section will be the starting point for considering the superconducting properties of Ti–Rh alloys.

4. Superconductivity

Kuentzler and Waterstrat [2] did not find superconductivity in the low-temperature Cu_3Au- and CuAuI-type structures above 1.4 K. To calculate the superconducting transition temperature T_c, first we shall consider the electron–phonon interaction. We base our discussion on the McMillan [15] formula in the generalized form for multicomponent compounds:

$$\lambda = \frac{1}{N_a} \sum_{i=1}^{N_a} \frac{N_i(E_F)\langle I^2\rangle_i}{M_i\langle\omega^2\rangle} \tag{1}$$

where N_a is the number of atoms in the unit cell; $\langle I^2\rangle_i$ is mean square electron–ion matrix element calculated within the rigid muffin-tin approximation (RMTA) [16]:

$$\langle I^2\rangle_i = \sum_l \frac{2l+2}{(2l+1)(2l+3)} (M_{l,l+1}^{(i)})^2 \frac{N_l^{(i)}(E_F)}{N_i(E_F)} \frac{N_{l+1}^{(i)}(E_F)}{N_i(E_F)}. \tag{2}$$

M_i is the ionic mass; $\langle\omega^2\rangle$ is the mean square phonon frequency defined by the electron–phonon $\alpha^2F(\omega)$ spectral function [15]

$$\langle\omega^2\rangle = \int_0^\infty \mathrm{d}\omega\, \omega\alpha^2F(\omega) \bigg/ \int_0^\infty \mathrm{d}\omega\, \omega^{-1}\alpha^2F(\omega).$$

$N_i(E_F)$ is the total DOS on the ith ion at the Fermi level E_F; $N_l^{(i)}(E_F)$ is the partial DOS on the ith ion for $E = E_F$; $M_{l,l+1}^{(i)}$ is partial electron–phonon matrix element [17] given by

$$\begin{aligned} M_{l,l+1}^{(i)} = \{[v^{(i)}(S_i) - E_F]S_i^2 \\ - (D_l^{(i)} - l)(D_{l+1}^{(i)} + l + 2)\}/S_i[(\partial D_l^{(i)}/\partial E)(\partial D_{l+1}^{(i)}/\partial E)]^{1/2} \end{aligned} \tag{3}$$

where $V^{(i)}(S_i)$ is the value of the potential at the Wigner–Seitz sphere radius S_i and $D_l^{(i)}$ is the logarithmic derivative of the wavefunction for the angular momentum quantum number l for $E = E_F$.

Equation (1) has a very convenient factorized form with electrons and phonons having independent contributions. The numerator, the electronic contribution, can be

Table 4. Mean square total and partial electron-ion matrix elements and the McMillan–Hopfield parameters for the low-temperature structures CuAuI and Cu_3Au of TiRh and $TiRh_3$, respectively.

	TiRh (CuAuI structure)		$TiRh_3$ (Cu_3Au structure)	
	Ti	Rh	Ti	Rh
$\langle I^2\rangle_{01}$ (au)	0.785×10^{-5}	2.101×10^{-5}	2.400×10^{-4}	2.074×10^{-5}
$\langle I^2\rangle_{12}$ (au)	1.699×10^{-5}	10.599×10^{-5}	4.209×10^{-5}	2.823×10^{-4}
$\langle I^2\rangle_{\text{total}}$(au)	2.484×10^{-5}	12.700×10^{-5}	2.881×10^{-4}	3.031×10^{-4}
η (Ryd au^{-2})	3.978×10^{-4}	6.668×10^{-4}	2.553×10^{-3}	1.223×10^{-2}
η (eV Å^{-2})	1.926×10^{-2}	3.229×10^{-2}	1.236×10^{-1}	5.920×10^{-1}

Table 5. The phonon characteristics Θ_D, $\omega_{\log}$ and $\langle\omega^2\rangle^{1/2}$ and the electron–electron interaction constant μ^*.

	TiRh (CuAuI structure)	$TiRh_3$ ($AuCu_3$ structure)
Θ_D (K)	383.0	526.0
$\langle\omega^2\rangle^{1/2}_{\min} = 0.56\Theta_D$ (K)	218.3	299.8
$\langle\omega^2\rangle^{1/2}_{\max} = 0.71\Theta_D$ (K)	271.9	373.5
$\omega^{\min}_{\log} = 0.87\langle\omega^2\rangle^{1/2}_{\min}$ (K)	189.9	260.8
$\omega^{\max}_{\log} = 0.87\langle\omega^2\rangle^{1/2}_{\max}$ (K)	236.6	324.9
μ^* (au)	0.073	0.081

expressed simply by parameters from the LMTO ASA formalism [9, 10, 17]. The electronic contributions of Ti and Rh, the McMillan–Hopfield parameter $\eta_i = N_i(E_F)\langle I^2\rangle_i$ as well as the partial contributions $\langle I^2\rangle^{(i)}_{l,l+1} \sim (M^{(i)}_{l,l+1})^2$ (see expression under summation in equation (2)) are collected together in table 4.

In the case of the phonon contribution (the denominator of equation (1)) the situation is more complicated. We have no information from experiment or theory on the phonon spectra. One can try to estimate $\langle\omega^2\rangle$ from the Debye temperature measurements [2]. The problem is that Θ_D, even if obtained accurately, is not a good measure of typical phonon frequencies, but only of the very lowest ones. Papaconstantopoulos *et al* [18] assumed that $\langle\omega^2\rangle = \frac{1}{2}\Theta_D^2$. Thus, when we compare $\langle\omega^2\rangle^{1/2}$ obtained from neutron scattering with Θ_D, we find that the ratio varies [19] from 0.57 to 0.71 for pure metals. That is why our calculated values of λ are given as values in the range $\langle\lambda_{\min}, \lambda_{\max}\rangle$. The mean phonon frequencies were estimated from the Debye temperatures obtained by Kuentzler and Waterstrat [2] (table 5). The values of λ are as follows: $\lambda_{\min} = 0.108$ and $\lambda_{\max} = 0.168$ for TiRh and, for $TiRh_3$, $\lambda_{\min} = 0.168$ and $\lambda_{\max} = 0.260$.

Using the value of the parameter λ, one can calculate the temperature of transition to the superconductivity based on the well known McMillan formula

$$T_c = C_i \exp\{-1.04(1+\lambda)/[\lambda - \mu^*(1+0.62\lambda)]\} \qquad (i = 1, 2, 3) \tag{4}$$

where the electron–electron interaction constant μ^* can be calculated using the formula of Bennemann and Garland [20] (table 5), and C_i is the multiplication factor: $C_1 = \Theta_D/1.45$ [14], $C_2 = \langle\omega^2\rangle^{1/2}/1.2$ [20], $C_3 = \omega_{\log}/1.2$ [21] and

$$\omega_{\log} = \exp\left(\frac{2}{\lambda}\int_0^\infty \frac{d\omega}{\omega}\, \alpha^2 F(\omega) \ln\omega\right)$$

calculated from $\omega_{\log} = 0.87\langle\omega^2\rangle^{1/2}$ as suggested by Buttler [19]. The values of $\omega_{\log}$ are

Table 6. The superconducting transition temperatures T_c for different factors used in equation (4) and for the extremal values λ_{min} and λ_{max} of electron–phonon coupling parameters, as well as for the experimental λ_{exp}, calculated for the $TiRh_3$ system.

	$TiRh_3$ ($AuCu_3$ structure)		
	$\lambda_{min} = 0.168$	$\lambda_{max} = 0.260$	$\lambda_{exp} = 0.329$
$\langle\omega^2\rangle^{1/2}_{min}$ (K)	48.16×10^{-6}	0.0929	0.528
$\langle\omega^2\rangle^{1/2}_{max}$ (K)	59.14×10^{-6}	0.1158	0.658
ω^{min}_{log} (K)	41.90×10^{-6}	0.0808	0.460
ω^{max}_{log} (K)	52.19×10^{-6}	0.1007	0.573
Θ_D (K)	68.92×10^{-6}	0.1349	0.926

given in table 5. The three above-mentioned factors have very similar values if we know the phonon spectrum from experiment or theory. Unfortunately we can use the approximate values only; so the results are different for distinct factors. Table 6 contains the values of T_c based on equation (4) for different factors C_i and the extremal electron–phonon coupling parameters λ_{min} and λ_{max} and also for λ_{exp} estimated from experimental data.

In the case of TiRh, T_c is very small, even for λ_{max} where $T_c \simeq 0.5 \times 10^{-6}$ K. The small value of T_c may change when we consider the tetragonal CuAuI-type structure. For $TiRh_3$ $T_c \simeq 0.5 \times 10^{-4}$ K for λ_{min} and $T_c \simeq 0.1$ K for λ_{max}. The exact values are presented in table 6. We see that the highest T_c are much smaller than 1 K, which is consistent with experiment [2] because the superconducting phase was not observed above 1.4 K. The electron–phonon coupling is very weak in these systems. The values of λ and T_c should be treated as approximate, especially because of the uncertainty of the phonon data. It is interesting to compare the values of λ calculated directly from the band structure and estimated from experiment. The experimental specific heat coefficient γ for $TiRh_3$ is equal to 11.4 mJ mol^{-1} K^{-2} [2]. Our calculated value $\gamma_0 = \frac{2}{3}\pi^2 k_B^2 N(E_F)$ is equal to 8.576 mJ mol^{-1} K^{-2}. Using the expression $\gamma = \gamma_0(1 + \lambda_{exp})$, one can obtain $\lambda_{exp} = 0.329$. Then $T_c(\lambda_{exp}) = 0.46$–$0.926$ K, depending on the factor used in equation (4) (see table 6). λ_{exp} is larger than λ_{max} by about 25%. We should not forget that λ_{exp} does not include the electron–phonon interaction only. The main contribution to λ_{exp} is from electron–phonon coupling but the above expression for γ is more general. In the experiment, λ_{exp} is an effective value which includes the influence of other phenomena which are able to enlarge the effective electronic mass such as spin fluctuations. The superconducting transition temperature is a rapidly varying function of the parameter λ, especially in the range of small values of λ. That is why the λ_{exp}-value obtained from specific heat measurement gives a T_c about six to seven times larger than for $\lambda_{max} = 0.260$ but even the highest T_c-value of 0.926 K is still below the limit of 1.4 K from the experiment of Kuentzler and Waterstrat [2].

5. Conclusions

In this paper the electronic and superconducting properties of ordered Ti–Rh alloys were considered. For simplicity we have performed calculations for the three cubic structures: Cu_3Au, CsCl and CuAuI. The LMTO ASA method was used for band calculations. We have obtained band structures along high-symmetry directions and the DOS.

The DOS for our systems have similar shapes to those for the related Zr–Rh alloys [5]. Using the RMTA we have calculated the electron–phonon coupling parameters for the two low-temperature structures: Cu_3Au and CuAuI. The maximal values for λ were 0.168 and 0.260 for TiRh (CuAuI structure) and $TiRh_3$ ($AuCu_3$ structure), respectively. The low values of λ gave low values of the superconducting transition temperatures T_c. For $TiRh_3$ the prediction was $T_c = 1$ K, which was not inconsistent with experiment [2].

Acknowledgments

The author is grateful to Professor J A Morkowski and Dr A Jezierski for stimulating discussions and for critically reading the manuscript. The calculations were performed using the programs of Dr N E Christensen. This work was supported by the Polish Academy of Sciences under Project CPBP 01.12.

References

[1] Kuentzler R and Waterstrat R M 1985 *Solid State Commun.* **54** 517
[2] Kuentzler R and Waterstrat R M 1988 *Solid State Commun.* **68** 85
[3] Yi S S, Chen B H and Franzen H F 1988 *J. Less-Common Met.* **143** 243
[4] Elliot R P 1965 *Constitution of Binary Alloys* (New York: Mc-Graw-Hill)
[5] Szajek A and Jezierski A 1989 *Solid State Commun.* **71** 917
[6] Watson R E, Weinert M, Davenport J W and Fernando G W 1989 *Phys. Rev.* B **39** 10761
[7] Watson R E, Weinert M, Davenport J W and Fernando G W 1988 *Scr. Metall.* **22** 1285
[8] Folkerts W and Haas C 1989 *J. Less-Common Met.* **147** 181
[9] Andersen O K 1975 *Phys. Rev.* B **12** 3060
[10] Skriver H L 1984 *The LMTO Method* (New York: Springer)
[11] Andersen O K, Jepsen O and Glötzel D 1985 *Highlights of Condensed Matter Theory* ed F Bassani, F Fumi and M P Tosi (Amsterdam: North-Holland)
[12] von Barth U and Hedin L 1972 *J. Phys. C: Solid State Phys.* **5** 1629
[13] Jepsen O and Andersen O K 1971 *Solid State Commun.* **9** 1763
[14] Lehman G and Taut M 1972 *Phys. Status Solidi* b **54** 469
[15] McMillan W L 1968 *Phys. Rev.* **167** 331
[16] Gaspari G D and Gyorffy B L 1972 *Phys. Rev. Lett.* **28** 801
[17] Pettifor D G 1977 *J. Phys. F: Met. Phys.* **7** 1009
[18] Papaconstantopoulos D A, Boyer L L, Klein B M, Williams A R, Moruzzi V L and Janak J F 1977 *Phys. Rev.* B **15** 4221
[19] Buttler W H 1977 *Phys. Rev.* B **15** 5267
[20] Benneman K H and Garland J W 1972 *Superconductivity in d and f Band Metals* ed D H Douglas (New York: American Institute of Physics) pp 103–37
[21] Dynes R C 1972 *Solid State Commun.* **10** 615
[22] Allen P B and Dynes R C 1975 *Phys. Rev.* B **12** 905